Transportation Research Part C 48 (2014) 453–467

Contents lists available at ScienceDirect

Transportation Research Part C

journal homepage: www.elsevier.com/locate/trc

A travel time reliability model of urban expressways with varying levels of service

Fangshu Lei [a], Yunpeng Wang [a], Guangquan Lu [a,*], Jianping Sun [b]

[a] Beijing Key Laboratory for Cooperative Vehicle Infrastructure Systems and Safety Control, Beihang University, Beijing 100191, China
[b] Beijing Transportation Research Center, Beijing 100073, China

ARTICLE INFO

Article history:
Received 30 April 2014
Received in revised form 25 September 2014
Accepted 30 September 2014
Available online 21 October 2014

Keywords:
Travel time reliability
Urban expressway
Travel time distribution
Travel distance
Level of service

ABSTRACT

Urban expressways usually experience several levels of service (LOS) because of the stop-and-go traffic flow caused by congestion. Moreover, multiple shock waves generate at different LOS interfaces. The dynamic of shock waves strongly influences the travel time reliability (TTR) of urban expressways. This study proposes a path TTR model that considers the dynamic of shock waves by using probability-based method to characterize the TTR of urban expressways with shock waves. Two model parameters are estimated, namely distribution of travel time (TT) per unit distance and travel distances in different LOS segments. Generalized extreme value distribution and generalized Pareto distribution are derived as distributions of TT per unit distance for six different LOS. Distribution parameters are estimated by using historical floating car data. Travel distances in different LOS segments are calculated based on shock wave theory. The range of TT along the path, which can help drivers arrange their trips, can be obtained from the TTR model. Finally, comparison is made among the proposed TTR model, generalized Pareto contrast model, which does not consider different LOS or existence of shock waves, and normal contrast model, which assumes TT per unit distance as normal distribution without considering shock wave. Results show that the proposed model achieves higher prediction accuracy and reduces the prediction range of TT. The conclusions can be further extended to TT prediction and assessment of measures to improve reliability of TT in a network.

1. Introduction

The most commonly considered measures in traffic reliability are connectivity reliability (Bell and Iida, 1997; Wakabayashi and Iida, 1992), capacity reliability (Chen et al., 1999), travel demand satisfaction reliability (Heydecker et al., 2007), and travel time reliability (TTR) (Asakura and Kashiwadani, 1991). TTR, which not only affects the daily travel of the public but also causes frustration among drivers, is a significant concern among travelers. As a result, a growing number of studies on TTR have been conducted (Asakura and Kashiwadani, 1991; Mahmassani et al., 2013; Turner et al., 1996).

Asakura and Kashiwadani (1991) first defined TTR as the probability of trips completed within a specified time in a given origin and destination (OD) at a certain level of service (LOS). Turner et al. (1996) defined TTR as the range of travel times (TT) experienced during a large number of daily trips. The 1998 California Transportation Plan further defined TTR as the variability between the expected TT or average TT and actual TT that results from the effects of non-recurrent congestion

* Corresponding author. Tel.: +86 10 82316330.
E-mail address: lugq@buaa.edu.cn (G. Lu).

http://dx.doi.org/10.1016/j.trc.2014.09.019
0968-090X/

(Mahmassani et al., 2013). The Future Strategic Highway Research Program (F-SHRP) Reliability Research Program (Cambridge Systematics, 2010) defined reliability as how TT vary over time (e.g., hour-to-hour or day-to-d ay). F-SHRP identified seven events that resulted in unreliability, such as incidents, adverse weather, work zones, special events, fluctuations in daily travel demand, and poorly coordinated traffic signals. The Federal Highway Administration (FHWA, 2014) formally defined TTR as the consistency or dependability in TT measured from day to day and/or across different times of the day.

Lomax et al. (2003) grouped TTR measures into three broad categories: (1) statistical range, which is the commonly used metric that employs standard deviation statistics to present an estimation of the range; (2) buffer time index (BTI), which is presented as either a percentage of the average trip time or value in minutes per mile or minutes of a typical trip; (3) tardy trip indicators, which use a threshold to identify an acceptable late arrival time with misery index as one of the indicators. van Lint et al. (2008) added the fourth category, which expresses the TTR in terms of probabilistic measures. Polus (1979) used the inverse of the standard deviation of TT distribution to estimate TTR. Chen et al. (2003) also used the standard deviation of TT distribution to represent the variability between the average TT and actual TT, which measures TTR. Carrion and Levinson (2013) used three measures of reliability. They incorporated these measures in the estimation of the route choice model. The three measures of reliability are standard deviation, shortened right range, and interquartile range (75–25%). Yao et al. (2014) assumed that the reliability of a link is weighted by the deviation of the TT of the link. They also applied TTR to transit network design. van Lint et al. (2008) denoted that the skew and width of TT distribution can represent the TTR and proposed the skew-width measure from a statistical perspective. Taylor (2012) computed BTI from the fitted TT Burr distribution parameters. Sumalee et al. (2013) used BTI and planning time index (PTI) to represent TTR with skew normal distribution of TT. Ng et al. (2011) assessed TTR with probability inequalities and free of TT distribution. Chen et al. (2013) considered TTR from a probabilistic perspective, and applied it to find reliable short paths. TTR also have been widely used in the field of route choice and traffic assignment (Coulombel and de Palma, 2014; Pattanamekar et al., 2003; Szeto et al., 2013) as well as in traffic network evaluation (Bhouri et al., 2013).

According to the FHWA (2014), among the emerging measures of TTR, only a few appear to have technical merit that are easily understood by non-technical audiences. Thus, the FHWA recommends the following four measures: (1) 90th or 95th percentile TT, which indicates how bad the delay will be on the heaviest travel days and regarded as the simplest measure of TTR. This measure has limitations because of the different lengths of most trips. (2) BTI, which represents the extra time that most travelers add to their average TT when planning trips to ensure on-time arrival. (3) PTI, which represents the total TT that should be planned when buffer time is considered. (4) Frequency that congestion exceeds a certain expected threshold, which is expressed as the percentage of days or time that TT exceed X minutes or travel speeds fall below Y mph. According to F-SHRP, many indicators are unreliable (Cambridge Systematics, 2010). BTI, which is widely used, is too unstable to be used as the primary reliability metric for tracking performance trends or studying the effects of improvements. van Lint et al. (2008) found the misery index unreliable in a particular period. Previous studies mentioned numerous factors that affect TTR, such as network structures (Yazici et al., 2012), network zones (Edwards and Fontaine, 2012) and driving behavior (Tu et al., 2012). However, traffic flow, which is an important aspect that is closely related to TTR, is often overlooked. Mahmassani et al. (2013) established a link between network traffic flow theory and TTR, with focus on a network fundamental diagram instead of TTR, and then used a standard deviation to represent TTR. At present, few TTR models consider the dynamics of shock wave effects on the TTR range.

Urban expressways usually experience several LOS because of the stop-and-go traffic flow caused by congestion. Moreover, traffic flow parameters vary in different LOS. Multiple shock waves are generated at different LOS interfaces. In addition, the length of each LOS is dynamic because of the propagation of shock waves. Therefore, the TTR of the expressway is strongly influenced by the dynamics of shock wave.

This paper proposes a path TTR model of urban expressways with different LOS by considering the dynamic effects of shock waves, based on the probabilistic method. It extends the TTR model to the path level instead of the link or segment level. The model is closely related to the distribution of TT. Besides, distributions of TT per unit distance in different LOS are also analyzed. Furthermore, travel distances in different LOS segments are calculated based on shock wave theory.

The paper is outlined as follows: Section 2 proposes the TTR model of urban expressways with different LOS and introduces the key parameters used in the model. Section 3 provides the estimation methods of the parameters based on real floating car data. Section 4 presents a case study and detailed discussion of the proposed model. Performance is made by comparing to the other two ones. Section 5 concludes the paper with future directions.

2. TTR Model of urban expressway with several LOS

The classic probability-based definition of TTR by Bell et al. (1997) has been adopted in this study. It is defined as the probability to complete a trip within a given time under a certain LOS. Let $r(T_{sum})$ be the TTR as follows:

$$r(T_{sum}) = p_r(T_{sum} \leqslant T_c|s) = \int_0^{T_c} f_r(T_{sum}|s)\mathrm{d}T_{sum} \tag{1}$$

where T_{sum} is the total TT of the expressway path; T_c is the path TT threshold depending on travel purpose; s is the traffic saturation, which is equal to the ratio of volume and capacity, denoting LOS; and $f_r(T_{sum}|s)$ is the probability density function (PDF) of the path TT.

As illustrated in Fig. 1, one vehicle (in red) travels through a path with length L on an urban expressway. The vehicle encounters n-LOS areas in the entire journey. Each LOS area is considered a single segment. Shock wave w_i exists with velocity $v_{s(i)}$ between the two LOS segments due to differences in traffic flow status. Hence, the vehicle needs to pass through $n-1$ shock waves with the dynamic length of each LOS segment, being made by the movement of shock waves. Total TT T_{sum} is the sum of the TT of the segments. T_i is the TT from the moment when the vehicle enters the path till meeting shock wave w_i. TT in ith LOS segment is $T_i - T_{i-1}$ (define $T_0 = 0$). When the vehicle enters the ith LOS segment, the distance between the vehicle and the shock front of w_i is $l_{0(i)}$, the distance between the shock fronts of w_i and w_{i+1} is $l_{D(i+1)}$, and so on. The actual distance traveled by the vehicle in the ith LOS segment is l_i. Assume that v_i is the average velocity of the vehicle in the ith LOS segment. The direction of v_1 is set as positive direction. This paper defines $i = 1, 2, 3, \ldots, n$ except when referring to the number of shock waves ($i = 1, 2, 3, \ldots, n-1$) by default.

It is assumed that the TT between segments are mutually independent, which is similar to the assumption of Yao et al. (2014). The total PDF of the first two segments is a convolution of the two segments' PDF. The PDF of the first three segments is a convolution of the first two segments' total PDF and the PDF of the third segment, and so on. The convolution process is shown in Fig. 2.

Accordingly, the following probability density of TT along the total urban expressway path can be determined as:

$$\begin{aligned} f_r(T_{sum}|S) &= [\ldots[[f_{r1}(T_1|s_1) * f_{r2}(T_2 - T_1|s_2)] * f_{r3}(T_3 - T_2|s_3)] * \ldots] * f_{rn}(T_{sum} - T_{n-1}|s_n) \\ &= \int_0^{T_n} \cdots \left[\int_0^{T_3} \left[\int_0^{T_2} f_{r1}(T_1|s_1) f_{r2}(T_2 - T_1|s_2) \mathrm{d}T_1 \right] \times f_{r3}(T_3 - T_2|s_3) \mathrm{d}T_2 \right] \times \ldots \times f_{rn}(T_{sum} - T_{n-1}|s_n) \mathrm{d}T_{n-1} \end{aligned} \quad (2)$$

for $T_0 = 0$, where $f_{ri}(T_i - T_{i-1}|s_i)$ is the PDF of TT in the ith segment, n is the number of LOS segments, s_i represents the LOS in the ith segment, and T_i is the TT from the period when the vehicle enters the path until it meets the ith shock front.

Based on the preceding equations, the TTR model can be obtained as follows:

$$\begin{aligned} r(T_{sum}) = \int_0^{T_c} \int_0^{T_n} \cdots \left[\int_0^{T_3} \left[\int_0^{T_2} f_{r1}(T_1|s_1) f_{r2}(T_2 - T_1|s_2) \mathrm{d}T_1 \right] \times f_{r3}(T_3 - T_2|s_3) dT_2 \right] \times \ldots \times f_{rn}(T_{sum} \\ - T_{n-1}|s_n) \mathrm{d}T_{n-1} \mathrm{d}T_{sum} \end{aligned} \quad (3)$$

The PDF $f_{ri}(T_i - T_{i-1}|s_i)$ need to be determined before estimating the TTR model for the expressway (Eq. (3)). Let t_i be the TT per unit distance (1 m) in the ith LOS. Then, the following equation can be obtained:

$$T_i - T_{i-1} = l_i t_i \quad (4)$$

The density function can be as follows:

$$f_{ri}(T_i - T_{i-1}|s_i) = f_{ri}(l_i t_i|s_i) \quad (5)$$

where l_i is the travel distance in the corresponding LOS segment.

In addition, two parameters are key to TTR estimation (in Section 3). One parameter is PDF of TT per unit distance $f_{ri}(t_i|s_i)$, which can be directly obtained from the distribution of TT per unit distance (in Section 3.1). The other parameter is travel distance l_i in the ith LOS segment, which is dynamic under the propagation of shock waves (in Section 3.2). The estimation methods of the two parameters are provided in the following two sections.

Note that distribution of TT per unit distance is adopted in this study instead of TT distribution of the entire path. The reason is explained as follows. It is known that the path TTR value is determined by the variation of speed and the length of the path. The distribution of TT of entire path is affected by the length of the path. The benefits of analyzing the distribution of TT per unit distance instead of entire path is that in this way the variability of TTR caused by the variation of travel speed can be thoroughly investigated. In addition, when the distribution of TT per unit distance is estimated, the PDF of TT in any path can be derived; while if the distribution of TT per path is adopted, we can only obtain the PDF of TT in one particular path. In order to get the PDF of other paths, the estimation process has to be repeated over and over. Taken together, the way of analyzing the distribution of TT per unit distance deals with a more general case.

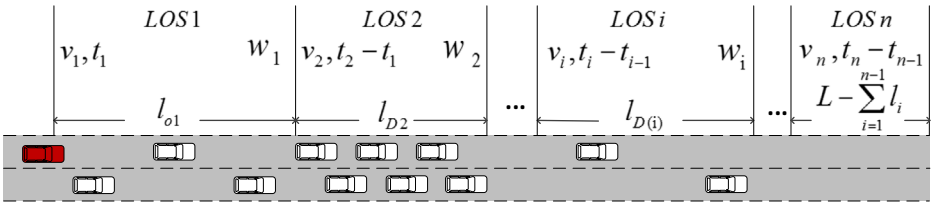

Fig. 1. Expressway traffic with shock waves.

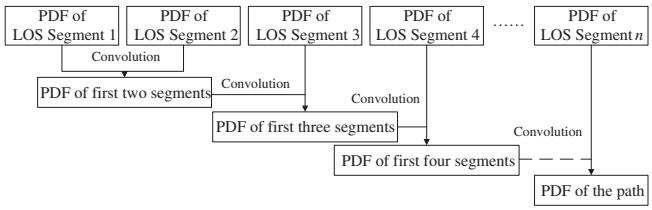

Fig. 2. Convolution process of path TT PDF estimation.

3. Model parameters

3.1. Distributions of TT per unit distance in different LOS

Definitions and measures of TTR vary in different studies. Nonetheless, all of them are closely related to the distribution of TT. The distribution of TT per unit distance is needed to obtain the PDF of TT per unit distance, which is a key input in the TTR model.

3.1.1. Data

This study used historical floating car data to fit the distribution of TT and estimate distribution parameters. The detailed information of floating car data is given as follows:

Data on Beijing's Third Ring Expressway from Xinxingqiao to Lizeqiao were collected, as shown with a bold line in Fig. 3. Data collection commenced at 0:00 AM on March 4, 2013, and ended at 23:59 PM on March 10, 2013, for a total of seven days. These data were aggregated at five-minute intervals and provide a rich source of TT and speed information.

The path from Xinxingqiao to Lizeqiao was divided into several segments in accordance with on- and off-ramps. The length of the segments was also obtained. Note that the speed data is time-mean average speed at every five minutes in each

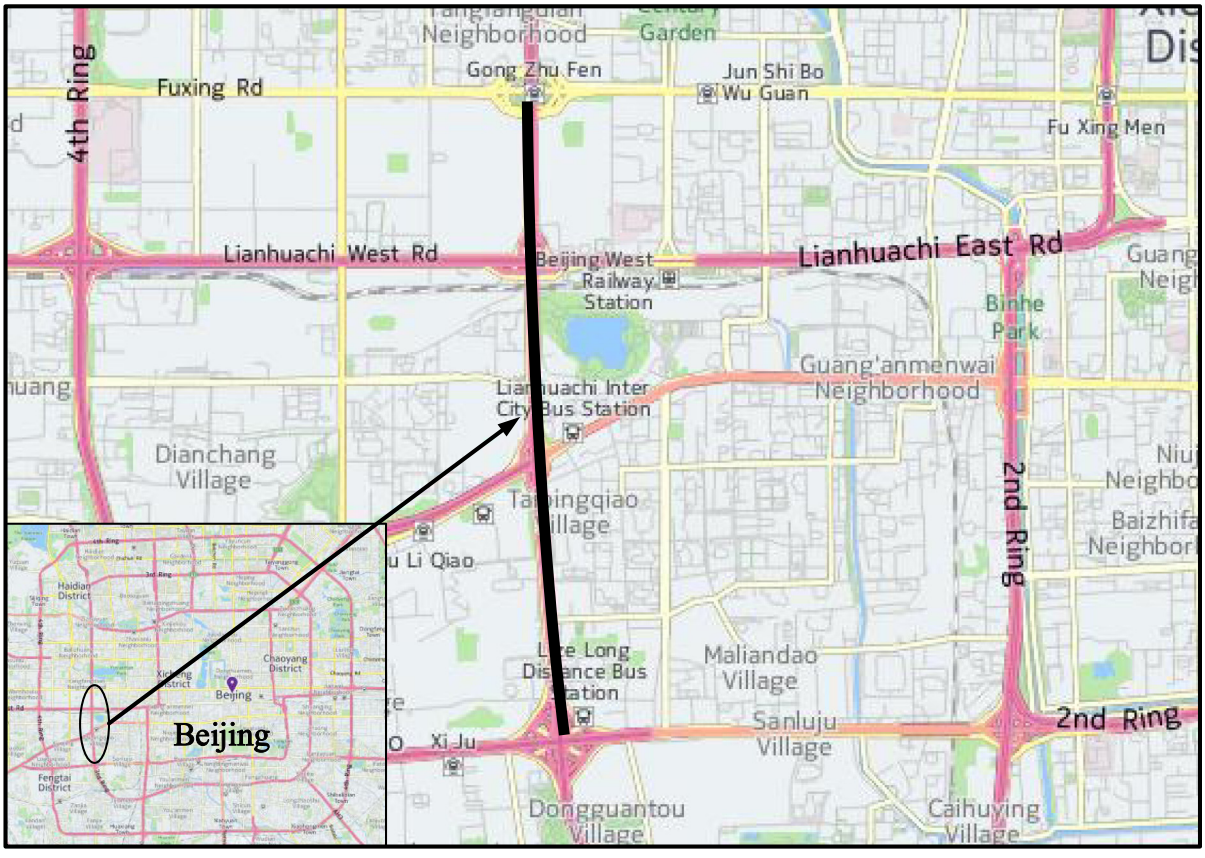

Fig. 3. Test bed for data acquisition.

segment. Considering the fact that space mean average speed can better characterize the state of the segments, the floating car time mean speeds were converted to the space mean speeds of each segment based on the time and space mean speed relationship (HCM, 2010).

$$v_{space} = 1.026 v_{time} - 3.035 \tag{6}$$

where v_{time} (km/h) is the time mean speed and v_{space} (km/h) is the space mean speed.

TT data were obtained from the speed data in addition to the information of segment length, and were mainly used in distribution and parameter estimations.

3.1.2. Distribution of TT per unit distance

Finite TT distributions are difficult to obtain. Lam and Small (2001) and Mahmassani et al. (2013) used mean and standard deviation to describe the distribution. The researchers use mean TT to estimate the standard deviation because of the difficulty in obtaining or predicting the standard deviation. Alvarez and Hadi (2012) and Chen et al. (2013) assumed TT to be symmetrically or normally distributed. However, empirical evidence (Fosgerau and Fukuda, 2012; van Lint and van Zuylen, 2005) showed that symmetrical distribution existed only in free-flow conditions and is considered unsuitable for congestion situations. Taylor (2012) used Burr distribution, which can describe the significant skewness of TT, to represent TT distribution and obtained desirable results. However, Taylor did not consider the different times of day or traffic flow status. Chen et al. (2013) assumed that each link has a random TT with a given distribution PDF, which also ignores the time-of-day or day-of-week variation.

This study considers the skewness of TT distribution and distinguishes six different distributions (or the same distribution with different parameter values) for six LOS. The method is similar to that used by van Lint et al. (2008), who considered four traffic conditions, namely, (1) free-flow conditions, (2) congestion onset, (3) congestion, and (4) congestion dissolution, and distinguished four shapes of TT distributions. Besides, this paper identifies a number of key characteristics of TT distribution based on empirical data, such as long right tails, which demonstrates the unreliability of TT.

The distribution of TT was estimated by using seven days of floating car historical data from the Third Ring Expressway. Similar to Hollander and Liu (2008), who used repeated simulation to estimate the distribution of TT, this paper adopted distribution of TT (s) per unit distance (1 m) to exclude the variability from travel distance. Suitable distributions were searched via the historical data in each LOS from numerous types of distributions. The p-value (Westfall, 1993) and K–S statistic (Koziol and Byar, 1975) were employed as the criteria to determine the optimal distribution. Taking LOS A as an example, all tested types of distributions and K–S statistics and *p*-values are shown in Table 1.

Table 2 shows the selected optimal distributions and distribution parameters. Distribution parameters were estimated by using maximum likelihood method.

For LOS A, TT per unit distance follows generalized extreme value distribution. By using the generalized extreme value PDF, the following equation can be obtained:

$$f(t_i; k_i, \mu_i, \sigma_i) = \frac{1}{\sigma_i}\left[1 + k_i\left(\frac{t_i - \mu_i}{\sigma_i}\right)\right]^{(-1/k_i)-1} \exp\left\{-\left[1 + k_i\left(\frac{t_i - \mu_i}{\sigma_i}\right)\right]^{-1/k_i}\right\} \tag{7}$$

Table 1
Distribution pool and K–S/*p*-value statistical results for LOS A.

Distribution	K–S statistic	*p*-value	Reject $\alpha = 0.05$ (critical value = 0.0563)
Generalized extreme value	0.0481	0.1317	No
Wakeby	0.0502	0.1036	No
Weibull (3P)	0.0519	0.0848	No
Kumaraswamy	0.0556	0.0535	No
Johnson SB	0.0559	0.0509	No
Burr	0.0600	0.0289	Yes
Beta	0.0760	0.0023	Yes
Dagum	0.0757	0.0024	Yes
Generalized Pareto	0.1078	0.0000	Yes
Weibull	0.1140	0.0000	Yes
Inverse Gaussian	0.1335	0.0000	Yes
Normal	0.1335	0.0000	Yes
Logistic	0.1340	0.0000	Yes
Gamma	0.1388	0.0000	Yes
Erlang	0.1449	0.0000	Yes
Lognormal	0.1413	0.0000	Yes
Pearson 6	0.1430	0.0000	Yes
Error	0.1569	0.0000	Yes
Uniform	0.1684	0.0000	Yes
Pareto	0.4550	0.0000	Yes

Table 2
Distribution selection of six LOS.

LOS	Distribution	K–S statistic	*p*-value	Parameter values		
				k	$\sigma(\times 10^{-2})$	$\mu(\times 10^{-2})$
A	Generalized extreme value	0.0481	0.1317	−0.8590	0.1951	4.8504
B	Generalized Pareto	0.0183	0.2564	−1.0731	1.5837	5.1102
C	Generalized Pareto	0.0110	0.7237	−0.6238	1.8975	6.6110
D	Generalized Pareto	0.0222	0.7638	−0.5529	1.6034	9.4480
E	Generalized Pareto	0.0270	0.8848	−0.7968	2.6498	12.0210
F	Generalized Pareto	0.0488	0.0373	−0.0447	9.7837	14.7430

for $1 + k_i(t_i - \mu_i)/\sigma_i > 0$, where $\mu_i \in R$ is the location parameter, $\sigma_i > 0$ is the scale parameter, and $k_i \in R$ is the shape parameter (Pitman, 1939).

For LOS B to LOS F, TT per unit distance follows generalized Pareto distribution. The following equation can be obtained for PDF:

$$f(t_i; k_i, \mu_i, \sigma_i) = \frac{1}{\sigma_i}\left[1 + k_i\left(\frac{t_i - \mu_i}{\sigma_i}\right)\right]^{(-1/k_i)-1} \tag{8}$$

for $t_i > \mu_i$ when $k_i > 0$, and $\mu_i \leqslant t_i \leqslant \mu_i - \sigma_i/k_i$ when $k_i < 0$, where $\mu_i \in R$ is the location parameter, $\sigma_i > 0$ is the scale parameter, and $k_i \in R$ is the shape parameter.

3.2. Travel distance in different LOS

The propagation of shock waves leads the distance of each LOS segment to be dynamic. The travel distance of vehicles in each LOS segment gets affected if two shock waves meet. Note that only the shock waves adjacent to the vehicles affect their travel distance. For instance, only the adjacent upstream shock wave $w_{\mathrm{up}.(i-1)}$ and downstream shock wave $w_{\mathrm{down}.i}$ affect the vehicles' travel distance in the ith LOS segment (Fig. 4).

Three situations have been considered depending on whether upstream or downstream shock waves meet.

3.2.1. Situation 1: No shock waves meet

Shock waves $w_{\mathrm{up}.(i-1)}$ or $w_{\mathrm{down}.i}$ do not meet (Fig. 5) while the vehicle travels in the ith LOS segment. The distance between the vehicle and $w_{\mathrm{down}.i}$ is $l_{0(i)}$ when the vehicle enters the ith LOS segment. Travel distance in the corresponding LOS segment is l_i. The vehicle passes the shock front at point p.

According to the definition of shock wave, the wave speed $v_{s(i)}$ can be calculated as follows:

$$v_{s(i)} = \frac{q_{i+1} - q_i}{k_{i+1} - k_i} = \frac{k_j \times (\bar{v}_{i+1} - \bar{v}_{i+1}^2/v_f) - k_j \times (\bar{v}_i - \bar{v}_i^2/v_f)}{k_j \times (\bar{v}_{i+1} - \bar{v}_{i+1}^2/v_f)/\bar{v}_{i+1} - k_j \times (\bar{v}_i - \bar{v}_i^2/v_f)/\bar{v}_i} = \bar{v}_i + \bar{v}_{i+1} - v_f \tag{9}$$

where k_i and q_i are the traffic flow parameters density and flow in the i$^{\mathrm{th}}$ LOS segment, respectively. $\bar{v}_i$ is the average speed in the i$^{\mathrm{th}}$ LOS segment. The traffic flow model (Eq. (10)) and Greenshields speed-flow relation (Eq. (11)) are adopted in Eq. (9).

$$q = kv \tag{10}$$

where k, v, and q are the traffic flow parameters, i.e., density, speed and flow, respectively.

$$q = k_j\left(v - \frac{v^2}{v_f}\right) \tag{11}$$

where k_j is jam density and v_f is free flow speed.

According to the traffic flow model in Eq. (10), there are $v_{s(i)} = \frac{\mathrm{d}q_i}{\mathrm{d}k_i} = v_i + k_i\frac{\mathrm{d}v_i}{\mathrm{d}k_i} \leqslant v_i$. If $v_i = v_{s(i)}$, $\mathrm{d}v_i = 0$, then shock waves will not exist. In the case of $v_i > v_{s(i)}$. TT in the ith LOS segment is calculated:

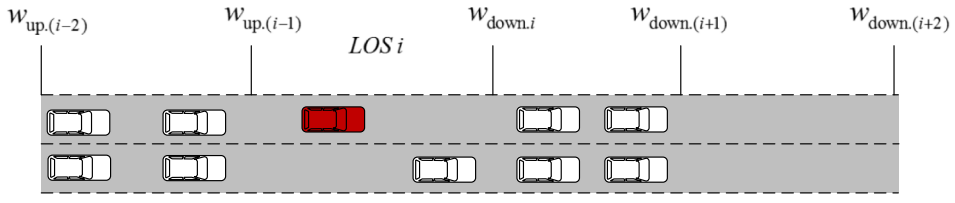

Fig. 4. Shock wave location diagram.

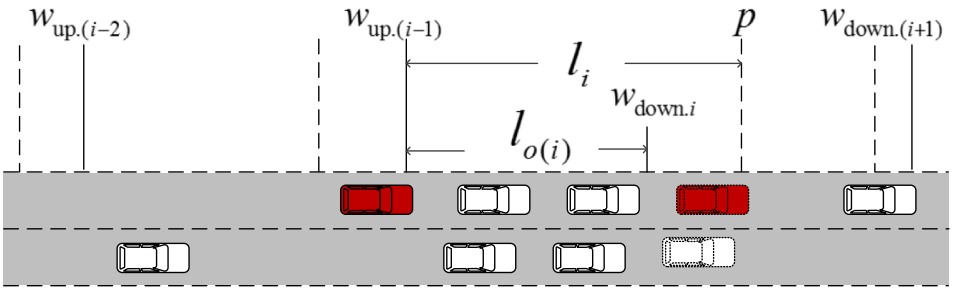

Fig. 5. No shock waves meet.

$$T_i - T_{i-1} = \frac{l_{o(i)}}{v_i - v_{s(i)}} \tag{12}$$

Accordingly, the travel distance of the vehicle in the ith LOS segment is calculated as follows:

$$\begin{cases} l_i = v_i \times (T_i - T_{i-1}) = \frac{v_i l_{o(i)}}{v_i + v_f - (\bar{v}_i + \bar{v}_{i+1})} & i = 1, 2, 3, \ldots, n-1 \\ l_i = L - l_1 - \ldots - l_{n-1}, & i = n \end{cases} \tag{13}$$

3.2.2. Situation 2: upstream shock waves meet

Fig. 6 illustrates the case when upstream shock waves $w_{up.(i-1)}$ and $w_{up.(i-2)}$ meet. Shock wave theory states that if traffic status A and B form shock wave x, and B and C form shock wave y, then traffic status A and C does not change when shock waves x and y meet at time t_0 (Fig. 7). Therefore, the meeting of the upstream shock waves does not affect traveling vehicles. The method used to calculate travel distance is the same as Situation 1. l_i can also be calculated by Eq. (12).

3.2.3. Situation 3: downstream shock waves meet

When downstream shock waves $w_{down.i}$ and $w_{down.(i+1)}$ meet, as illustrated in Fig. 8, a new shock wave $w_{down.(i)(i+1)}$ will be formed at point q (Fig. 8) while the vehicle travels in the upstream LOS segment. In this case, the shock wave $w_{down.(i+2)}$ and the newly formed shock wave $w_{down.(i)(i+1)}$ are the next two downstream shock waves of the vehicle. Supposing that m downstream shock waves meet ($m \geqslant 2$) when the vehicle travels in the ith LOS segment, the vehicle passes the final formed shock wave $w_{s(i)(i+1)\ldots(i+m-1)}$ at point p.

Based on Eq. (9), the wave speed of the shock wave $w_{s(i)(i+1)\ldots(i+m-1)}$ is $v_{s(i)(i+1)\ldots(i+m-1)}$, which is determined as follows:

$$v_{s(i)(i+1)\ldots(i+m-1)} = \bar{v}_i + \bar{v}_{i+m} - v_f \tag{14}$$

Based on the travel distance relationships between the vehicle and ith shock front as well as the vehicle and the newly formed shock front, the TT in each part can be determined by using the following equations:

$$l_{D(i+m-1)} = (v_{s(i)(i+1)\cdots(i+m-2)} - v_{s(i+m-1)}) \cdot T_{i.(m-1)} \tag{15}$$

$$v_{s(i)} \cdot T_{i.1} + \ldots + v_{s(i)(i+1)\ldots(i+m-2)} \cdot T_{i.(m-1)} + l_{o(i)} - v_i \cdot (T_{i.1} + \ldots + T_{i.(m-1)}) = (v_i - v_{s(i)(i+1)\ldots(i+m-1)}) \cdot T_{i.m} \tag{16}$$

where $T_{i.1}$ is the time from the period when the vehicle enters the ith LOS segment (at point e, as shown in Fig. 8) till the meeting of the next two downstream shock waves (first-time meeting, at point q), $T_{i.2}$ is the time between the first-time meeting of shock wave and second-time meeting of shock wave, and so on. $T_{i.m-1}$ is the time between the *(m–2)-time*

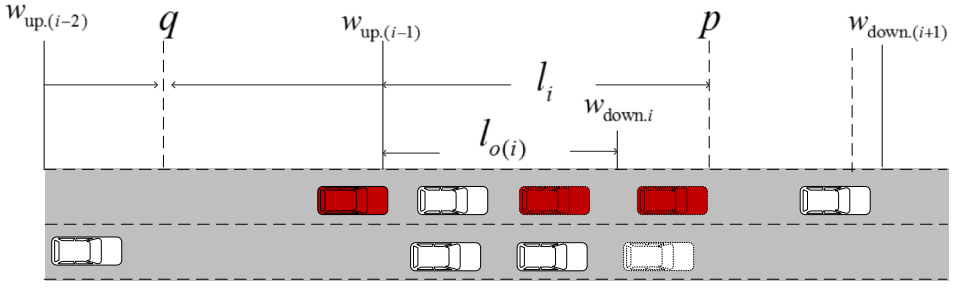

Fig. 6. Upstream shock waves meet.

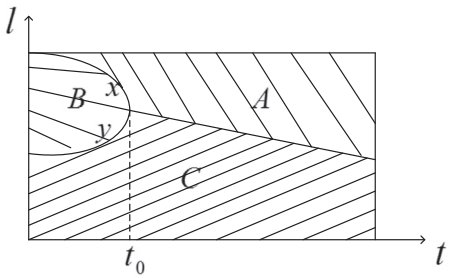

Fig. 7. Traffic characteristic curve.

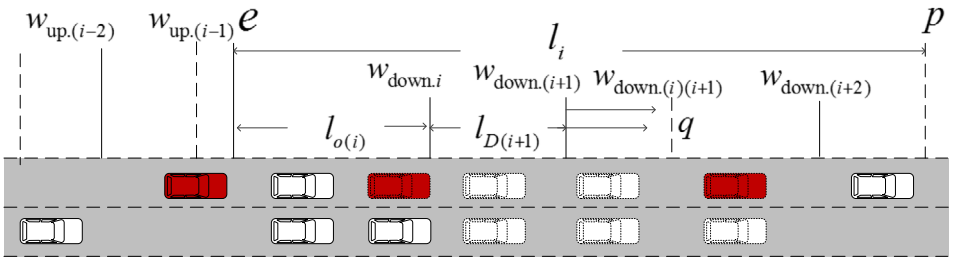

Fig. 8. Downstream shock waves meet.

meeting of shock wave and *(m−1)-time* meeting of shock wave, and $T_{i,m}$ is the time between the *(m−1)-time* meeting of shock wave and the vehicle passing the last newly formed shock wave (at point *p*).

The total TT of the vehicle in the ith LOS segment is as follows:

$$T_{i.1} + T_{i.2} + \ldots + T_{i.m} = T_i - T_{i-1} \tag{17}$$

Based on Eqs. (14)–(17), the travel distance of the vehicle in the ith LOS segment is calculated as:

$$\begin{cases} l_i = v_i \cdot (T_i - T_{i-1}) = v_i \cdot \left(\frac{l_{o(i)} + l_{D(i+1)} \cdot (\bar{v}_{i+1} - \bar{v}_{i+m})/(\bar{v}_i - \bar{v}_{i+2}) + \ldots + l_{D(i+m-1)} \cdot (\bar{v}_{i+m-1} - \bar{v}_{i+m})/(\bar{v}_i - \bar{v}_{i+m})}{v_i - \bar{v}_i - \bar{v}_{i+m} + v_f} \right), & i = 1, 2, 3, \ldots, n-1 \\ l_i = L - l_1 - \ldots - l_{n-1}, & i = n \end{cases} \tag{18}$$

where $\bar{v}_i \neq \bar{v}_{i+m}$. No *m* shock waves meet when $\bar{v}_i = \bar{v}_{i+m}$.

3.2.4. Determining the situation

In real case, under which situation to calculate the travel distance in the corresponding LOS segment needs to be identified.

When a vehicle travels through a certain LOS segment and *m* downstream shock waves meet according to travel distance relationship, the following equation is obtained:

$$v_i(T_{i.1} + T_{i.2} + \ldots + T_{i.(m-1)}) \leqslant l_{o(i)} + v_{s(i)} T_{i.1} + v_{s(i)(i+1)} T_{i.2} + \ldots + v_{s(i)(i+1)\ldots(i+m-2)} T_{i.(m-1)} \tag{19}$$

According to Eqs. (13)–(15) and (18), the following equation is obtained:

$$\frac{v_i - \bar{v}_i - \bar{v}_{i+1} + v_f}{\bar{v}_i - \bar{v}_{i+2}} l_{D(i+1)} + \frac{v_i - \bar{v}_i - \bar{v}_{i+2} + v_f}{\bar{v}_i - \bar{v}_{i+3}} l_{D(i+2)} + \ldots + \frac{v_i - \bar{v}_i - \bar{v}_{i+m-1} + v_f}{\bar{v}_i - \bar{v}_{i+m}} l_{D(i+m-1)} \leqslant l_{o(i)} \tag{20}$$

where $\bar{v}_i \neq \bar{v}_{i+2}$. In contrast to Eq. (20) or $\bar{v}_i = \bar{v}_{i+2}$, no *m* shock waves meet.

Eq. (20) (*m* = 2) is used to determine whether the next two shock waves downstream meet when the vehicle goes through the ith LOS segment area. If not, the same steps in the next LOS segment area are performed. If so, the total number *m* of shock waves met is calculated by using Eqs. (20) and (21). Then, return to Eq. (20) (*m* = 2) to determine the (*i* + 1)th LOS segment.

$$\frac{v_i - \bar{v}_i - \bar{v}_{i+1} + v_f}{\bar{v}_i - \bar{v}_{i+2}} l_{D(i+1)} + \frac{v_i - \bar{v}_i - \bar{v}_{i+2} + v_f}{\bar{v}_i - \bar{v}_{i+3}} l_{D(i+2)} + \ldots + \frac{v_i - \bar{v}_i - \bar{v}_{i+m-1} + v_f}{\bar{v}_i - \bar{v}_{i+m}} l_{D(i+m-1)} + \frac{v_i - \bar{v}_i - \bar{v}_{i+m} + v_f}{\bar{v}_i - \bar{v}_{i+m+1}} l_{D(i+m)} > l_{o(i)} \tag{21}$$

Fig. 9 shows the calculation process of the entire travel distance.

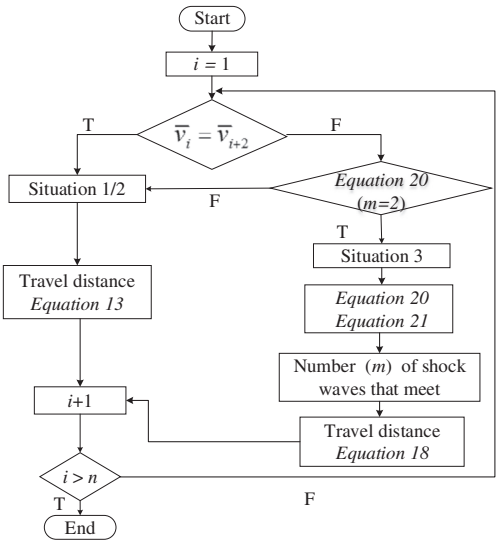

Fig. 9. Flowchart of travel distance calculation.

By using distributions of TT per unit distance and the estimation results of travel distance, the following equation is obtained:

$$f_{ri}(T_i - T_{i-1}|s_i) = f(T_i - T_{i-1}; k_i, l_i\mu_i, l_i\sigma_i) = \frac{1}{l_i\sigma_i}\left[1 + k_i\left(\frac{(T_i - T_{i-1}) - l_i\mu_i}{l_i\sigma_i}\right)\right]^{(-1/k_i)-1} \exp\left\{-\left[1 + k_i\left(\frac{(T_i - T_{i-1}) - l_i\mu_i}{l_i\sigma_i}\right)\right]^{-1/k_i}\right\} \quad (22)$$

or

$$f_{ri}(T_i - T_{i-1}|s_i) = f(T_i - T_{i-1}; k_i, l_i\mu_i, l_i\sigma_i) = \frac{1}{l_i\sigma_i}\left[1 + k_i\left(\frac{(T_i - T_{i-1}) - l_i\mu_i}{l_i\sigma_i}\right)\right]^{(-1/k_i)-1} \quad (23)$$

where k_i, μ_i, and σ_i are distributions of TT per unit distance parameters, which have been estimated (refer to Table 2). l_i is the travel distance in each LOS segment, which has been calculated (refer to Fig. 9). Eq. (22) is used for LOS A, and Eq. (23) is used for LOS B-F. Then the TTR model (in Eq. (3)) can be obtained.

4. Analysis and discussion

4.1. Case study

Four LOS segments (LOS C, LOS F, LOS D, and LOS E) were taken as examples to explain the TTR model this paper has proposed. Modeling parameters are set as follows: the average speeds of the four LOS segments are $\bar{v}_1 = 13.3$ m/s, $\bar{v}_2 = 6.1$ m/s, $\bar{v}_3 = 10$ m/s, and $\bar{v}_4 = 8.1$ m/s, respectively. These speeds were calculated based on the velocity boundary of the LOS class according to the Highway Capacity Manual (HCM) (2010). The free-flow speed v_f was calculated based on the 90th percentile value (FHWA, 2014) of travel speeds within seven days on the Third Ring Expressway. The results show that the value is $v_f = 19$ m/s. The expressway path length is $L = 4$km. The initial values of the LOS segments are $l_{o(1)} = l_{D(2)} = l_{D(3)} = l_{D(4)} = 1$ km. Table 2 shows the distribution of TT per unit distance parameter values. The actual travel distances were calculated by following the flowchart in Fig. 9. The following detailed demonstration is provided to explain the calculation process of deriving the travel distances at different LOS segments (Section 3.2):

(1) $\bar{v}_1 \neq \bar{v}_2 \neq \bar{v}_3 \neq \bar{v}_4$ are determined.
(2) A vehicle enters the first LOS C segment with velocity v_1 (14 m/s, for example), which is obtained from the floating car data corresponding to LOS C speed. Then, Eq. (20) ($m = 2$) is used to determine whether the next two shock waves between LOS C and F and between LOS F and D meet. If the equation holds, the next two shock waves meet. The results show that Eq. (20) does not hold, which means that, the next two shock waves do not meet. Therefore, Eq. (13) is used to calculate the travel distance in the LOS C segment. The result is $l_1 = 1029.4$ m.
(3) Then, the vehicle enters LOS F segment with velocity v_2 (5 m/s, for example), and the same process is repeated with Eq. (20) ($m = 2$). The results show that Eq. (20) holds, which means that, the shock waves between LOS F and D and between LOS D and E meet.

(4) Eqs. (20) and (21) are used to determine parameter m The calculation result is $m = 2$. Therefore, Eq. (18) is used to calculate the travel distance in the LOS F segment. The result is $l_2 = 994.9$ m.
(5) Due to the meeting of the shock waves, the vehicle does not go through LOS D. The travel distance in the LOS E segment is $l_3 = L - l_1 - l_2 = 1975.7$ m .

Fig. 10 shows the TTR modeling result. An instance occurs in which the shock waves meet and the vehicle travels through three LOS segments, namely, LOS C, LOS F, and LOS E. The path TTR curve is more unreliable than any single segment. The TT range in the path can be obtained from the TTR curve. This range is within 408 s to 660 s. The results can help drivers get informed of the potential TT variation and make appropriate arrangement about their trips.

Probability density curves (Fig. 11) show the skewness or long right tails of TT distributions, which agree well with the results by Taylor (2012) and van Lint et al. (2008). It can also be observed that TT distributions under lower LOS have a heavier skew.

4.2. Discussion

The practicability of the proposed TTR model was discussed through a comparison with other commonly utilized TTR models. The floating car data at five-minute intervals were considered too long to be used in the proposed TTR model. Historical GPS data at 14 to 17-s intervals with speed, TT, and travel distance information were used in the comparison. The GPS data have the same location and time as the floating car data, which are on the Third Ring Expressway from Xinxingqiao to Lizeqiao (Fig. 3) from March 4 to 10, 2013. A total of 44 groups of suitable data have been selected in the entire database. Thus, 44 groups of estimation results have been made for comparison. The three models were employed for this purpose:

(1) The TTR model proposed in this study.
(2) Generalized Pareto contrast model, which models TTR according to probability-based definition but does not consider different LOS or existence of shock waves. Per unit distance TT was considered to follow generalized Pareto distribution. Generalized extreme value distribution was not considered here because most of the empirical speed data obtained were not corresponding to LOS A, and most of the distributions used in the TTR model are generalized Pareto distributions. The generalized Pareto contrast model is given as:

$$p_r(t \leqslant t_c|s) = \int_0^{t_c} f_r(t|s)dt = \int_0^{t_c} \frac{1}{L\sigma}\left[1 + k\left(\frac{t - L\mu}{L\sigma}\right)\right]^{(-1/k)-1} dt \tag{24}$$

where L is the length of the entire path, and k, σ, μ are generalized Pareto distribution parameters of TT per unit distance of the entire path.

(3) Normal contrast model, which also models TTR according to probability-based definition and does not consider different LOS or existence of shock waves. With per unit distance TT considered to be normal distribution, which is the most commonly used method to describe TT distribution (Alvarez and Hadi, 2012; Rakha et al., 2010), the normal contrast model is given as:

$$p_r(t \leqslant t_c|s) = \int_0^{t_c} f_r(t|s)dt = \Phi\left(\frac{t_c - L\bar{t}}{L^2\sigma^2}\right) \tag{25}$$

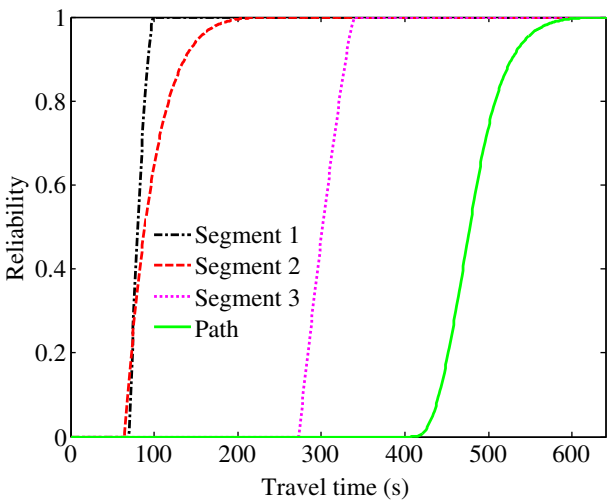

Fig. 10. Simulation results of TTR curve.

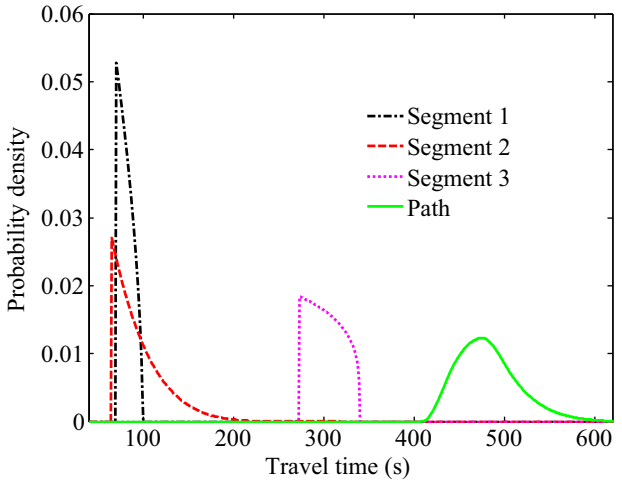

Fig. 11. Simulation results of probability densities.

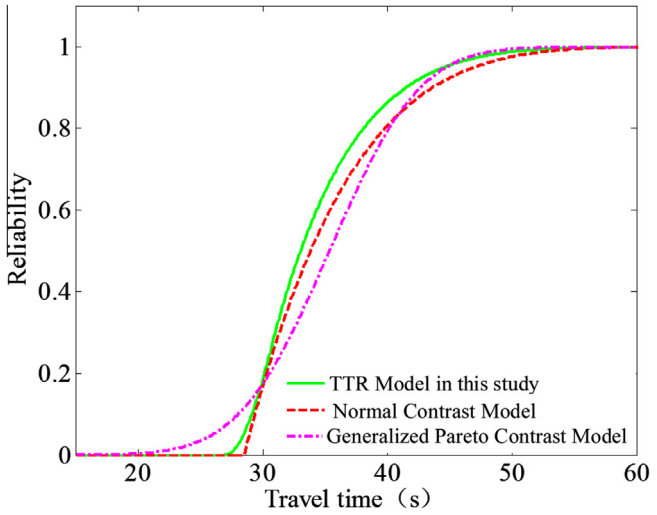

Fig. 12. Comparison of reliability by three TTR models.

where L is the length of the entire path; $\bar{t}$ and σ^2 are the mean and variance of the TT per unit distance of the entire path, respectively.

Fig. 12 illustrates an example of comparison results by three TTR models. It shows that the reliability value by proposed TTR model is slightly higher than by the other two contrast models after TT is higher than 30s. Besides, the probability densities of the three models were compared to demonstrate the improvement of the accuracy achieved by the proposed TTR model, as shown in Fig. 13.

The maximum TT probability density value is defined as the predicted TT in this paper, namely, μ_1 in the proposed TTR model, μ_2 in the generalized Pareto contrast model, and μ_3 in the normal contrast model, respectively. It is defined that the difference between predicted TT and actual TT is deviation value, namely, δ_1, δ_2, and δ_3 for the three models, respectively (Fig. 13). Therefore, smaller deviation values denote more accurate prediction.

The statistical results of 44 groups of comparison tests are presented in Figs. 14–16, and Table 3.

(1) Fig. 14 shows the 44 groups of tests results. Figs. 15 and 16 show the deviation difference between the proposed TTR model and two contrast models, respectively. The bars above the horizontal axis indicate that the deviation values by the contrast model are higher than those by the proposed TTR model. Therefore, it concludes that the proposed TTR model provides more accurate prediction results than both generalized Pareto contrast model and normal contrast model.

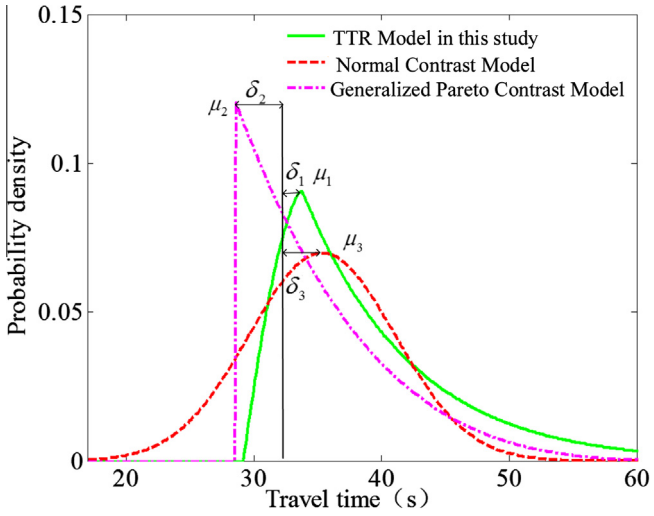

Fig. 13. Comparison of probability densities by three TTR models.

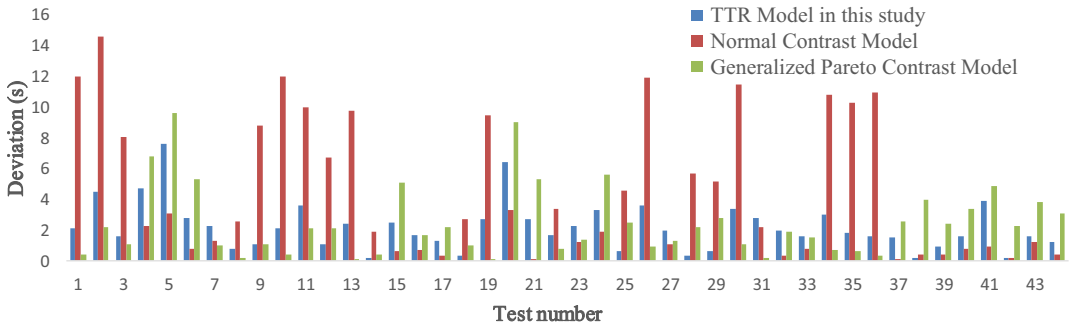

Fig. 14. Comparison of deviation values.

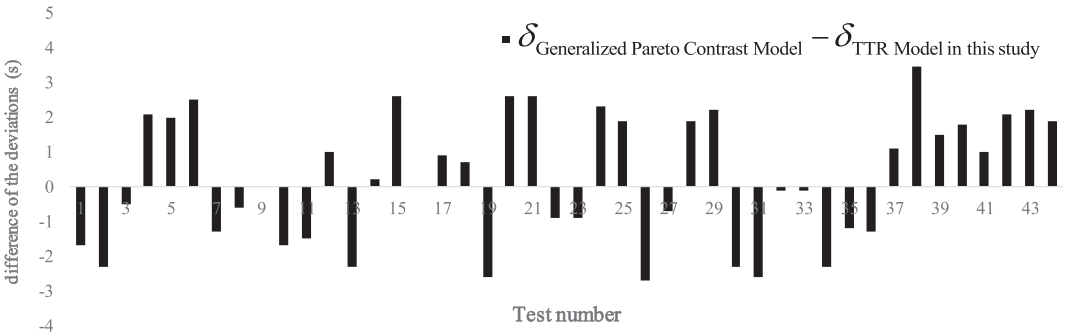

Fig. 15. Difference of the deviation of generalized Pareto contrast model and proposed TTR model.

(2) The summation of deviation values given by the proposed TTR model deviation is 96.2 s, which is lower than those by the generalized Pareto contrast model (107.5 s) and normal contrast model (197.5 s). Similarly, the mean deviation by the proposed model is 2.2 s lower than those by the generalized Pareto model (2.5 s) and normal contrast model (4.5 s).

(3) For 80 percentile values, the deviation given by the proposed TTR model is less than 3.0 s, while the deviation by the generalized Pareto contrast model is 3.8 s and that of the normal contrast model is as high as 9.8 s, as shown in the following:

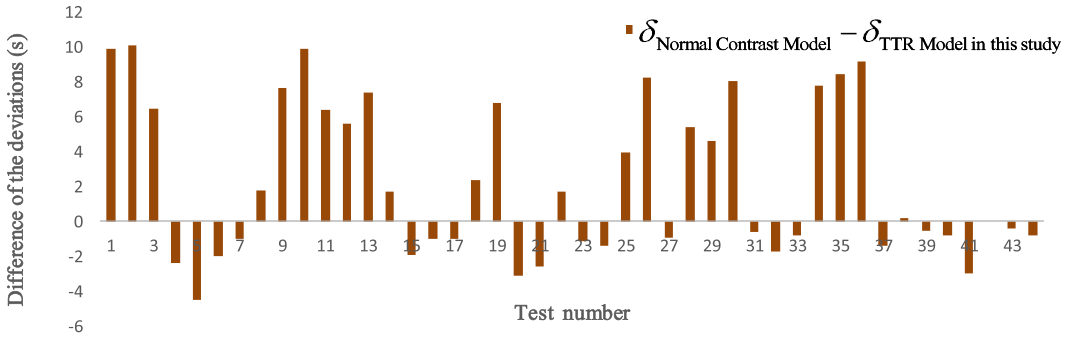

Fig. 16. Difference of the deviation of normal contrast model and proposed TTR model.

Table 3
Comparison results of deviation values.

	Proposed TTR model (s)	Generalized pareto contrast model (s)	Normal contrast model (s)
Sum	96.2	107.5	197.5
Mean	2.2	2.5	4.5
80 percentile	3.0	3.8	9.8

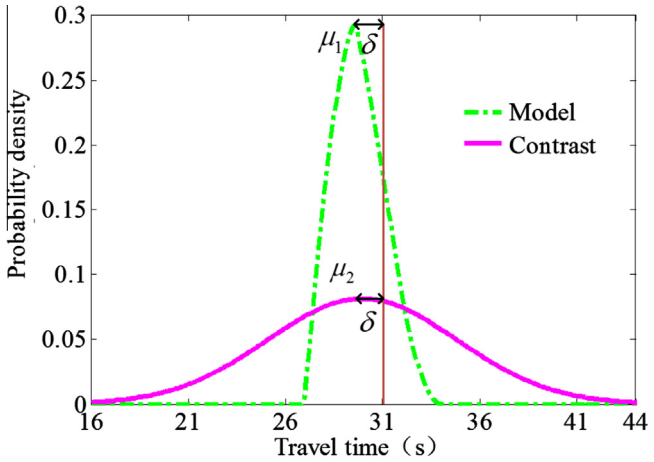

Fig. 17. Predicted range of TT.

$$P(t < \mu_1 \pm \delta_1) = P(t < \mu_2 \pm \delta_2) = P(t < \mu_3 \pm \delta_3) = 0.8 \tag{26}$$

$$\delta_1 = 3.0\ \text{s} \quad \delta_2 = 9.8\ \text{s} \quad \delta_3 = 3.8\ \text{s} \tag{27}$$

(4) The comparison results show that the generalized Pareto contrast model performs better than the normal contrast model. It indicates that the generalized Pareto distribution used in this study has better performance than normal distribution in characterizing TT.
(5) A comparison between the TTR model and normal contrast model indicates that even when deviations δ in the TTR model and the normal contrast model are close to each other, the proposed TTR model significantly reduces the prediction range (Fig. 17).

In summary, the above results demonstrate that the TTR model proposed in this study achieves desirable prediction accuracy and help reduce the prediction range of TT, which has important practical significance in TTR estimation.

5. Conclusion

This study was motivated by real-life situations in many major cities, which experience frequent traffic congestions. The congestions bring extra TT to travelers. Most travelers, especially commuters, are less tolerant of unexpected delays.

Moreover, these travelers prefer 'reliable' travel to 'a short time' travel. Therefore, this paper aims to estimate the TTR on urban expressways with variable traffic conditions in several LOS due to the stop-and-go traffic flow caused by congestion. Shock waves are generated at different LOS interfaces. In addition, the TTR of the expressway is strongly influenced by the dynamics of shock waves.

A path TTR model was proposed to consider the dynamics of shock waves by using probability-based methods to characterize the TTR of urban expressways with shock waves. Moreover, the path probability density function in the model was calculated using the convolution method. Two parameters in the TTR model were estimated. First, varying traffic statuses at different times of day were considered. Six different TT distributions (or the same distribution with different parameter values) were used for six LOS. Generalized extreme value and generalized Pareto distribution were derived as distributions of TT per unit distance for different LOS. Distribution parameters were estimated based on historical floating car data by using maximum likelihood method. Second, the travel distances in different LOS were calculated based on shock wave theory. The TTR model was used to obtain the TT range of the path, which can help drivers arrange trips. Furthermore, a comparison was made among the proposed the TTR model, generalized Pareto contrast model, and normal contrast model. Generalized Pareto contrast model does not consider different LOS or existence of shock waves. Normal contrast model assumes TT per unit distance as normal distribution without considering shock wave. The analysis results indicate that the proposed model achieves desirable prediction accuracy and reduce the prediction range of TT. In future studies, the TTR model can be further optimized by considering the connection between upstream and downstream segments.

The prominent features of this study are the presentation of a useful tool for accurate TTR estimation and the proposal of different distributions of TT per unit distance for different LOS. The computational results are satisfactory and show the effectiveness of the proposed method. This study also provides support for TT prediction and user equilibrium path flow estimation. The proposed TTR model can be further extended to TT prediction and assessment of measures to improve the reliability of travel in a network.

Acknowledgment

The authors would like to express our gratitude to the Beijing Transportation Research Center for providing the floating car data. This study is supported by the National Basic Research Program of China (2012CB725404).

Reference

Alvarez, P., Hadi, M., 2012. Time-variant travel time distributions and reliability metrics and their utility in reliability assessments. Transp. Res. Rec.: J. Transp. Res. Board 2315 (1), 81–88.
Asakura, Y., Kashiwadani, M., 1991. Road Network Reliability Caused by Daily Fluctuation of Traffic Flow, PTRC Summer Annual Meeting, 19th, 1991. University of Sussex, United Kingdom.
Bell, M.G., Iida, Y., 1997. Transportation network analysis, New Jersey.
Bell, M.G., Shield, C.M., Busch, F., Kruse, G., 1997. A stochastic user equilibrium path flow estimator. Transp. Res. Part C: Emerging Technol. 5 (3), 197–210.
Bhouri, N., Haj-Salem, H., Kauppila, J., 2013. Isolated versus coordinated ramp metering: field evaluation results of travel time reliability and traffic impact. Transp. Res. Part C: Emerging Technol. 28, 155–167.
Cambridge Systematics, 2010. Analytical procedures for determining the impacts of reliability mitigation strategies, report for NCHRP SHRP 2 project L03. <http://onlinepubs.trb.org/onlinepubs/f-shrp/f-shrp_webdoc_3.pdf>.
Carrion, C., Levinson, D., 2013. Valuation of travel time reliability from a GPS-based experimental design. Transp. Res. Part C: Emerging Technol. 35, 305–323.
Chen, A., Yang, H., Lo, H.K., Tang, W.H., 1999. A capacity related reliability for transportation networks. J. Adv. Transp. 33 (2), 183–200.
Chen, B.Y., Lam, W.H., Sumalee, A., Li, Q., Shao, H., Fang, Z., 2013. Finding reliable shortest paths in road networks under uncertainty. Networks Spatial Econ. 13 (2), 123–148.
Chen, C., Skabardonis, A., Varaiya, P., 2003. Travel-time reliability as a measure of service. Transp. Res. Rec.: J. Transp. Res. Board 1855 (1), 74–79.
Coulombel, N., de Palma, A., 2014. The marginal social cost of travel time variability. Transp. Res. Part C: Emerging Technologies.
Edwards, M.B., Fontaine, M.D., 2012. Investigation of travel time reliability in work zones with private-sector data. Transp. Res. Rec.: J. Transp. Res. Board 2272 (1), 9–18.
FHWA, 2014. Travel time reliability: making it there on time, all the time. <http://ops.fhwa.dot.gov/publications/tt_reliability/TTR_Report.htm>.
Fosgerau, M., Fukuda, D., 2012. Valuing travel time variability: characteristics of the travel time distribution on an urban road. Transp. Res. Part C: Emerging Technol. 24, 83–101.
HCM, 2010. Highway Capacity Manual. Washington, DC.
Heydecker, B., Lam, W.H., Zhang, N., 2007. Use of travel demand satisfaction to assess road network reliability. Transportmetrica 3 (2), 139–171.
Hollander, Y., Liu, R., 2008. Estimation of the distribution of travel times by repeated simulation. Transp. Res. Part C: Emerging Technol. 16 (2), 212–231.
Koziol, J.A., Byar, D.P., 1975. Percentage points of the asymptotic distributions of one and two sample KS statistics for truncated or censored data. Technometrics 17 (4), 507–510.
Lam, T.C., Small, K.A., 2001. The value of time and reliability: measurement from a value pricing experiment. Transp. Res. Part E: Logist. Transp. Rev. 37 (2), 231–251.
Lomax, T., Schrank, D., Turner, S., Margiotta, R., 2003. Selecting Travel Reliability Measures. Texas Transportation Institute Monograph.
Mahmassani, H., Hou, T., Saberi, M., 2013. Connecting network-wide travel time reliability and the network fundamental diagram of traffic flow. Transp. Res. Rec.: J. Transp. Res. Board 2391 (2), 80–91.
Ng, M., Szeto, W., Travis Waller, S., 2011. Distribution-free travel time reliability assessment with probability inequalities. Transp. Res. Part B: Methodol. 45 (6), 852–866.
Pattanamekar, P., Park, D., Rilett, L.R., Lee, J., Lee, C., 2003. Dynamic and stochastic shortest path in transportation networks with two components of travel time uncertainty. Transp. Res. Part C: Emerging Technol. 11 (5), 331–354.
Pitman, E., 1939. Tests of hypotheses concerning location and scale parameters. Biometrika, 200–215.
Polus, A., 1979. A study of travel time and reliability on arterial routes. Transportation 8 (2), 141–151.
Rakha, H., El-Shawarby, I., Arafeh, M., 2010. Trip travel-time reliability: issues and proposed solutions. J. Intell. Transp. Syst. 14 (4), 232–250.

Sumalee, A., Pan, T., Zhong, R., Uno, N., Indra-Payoong, N., 2013. Dynamic stochastic journey time estimation and reliability analysis using stochastic cell transmission model: algorithm and case studies. Transp. Res. Part C: Emerging Technol. 35, 263–285.
Szeto, W., Jiang, Y., Wong, K., Solayappan, M., 2013. Reliability-based stochastic transit assignment with capacity constraints: formulation and solution method. Transp. Res. Part C: Emerging Technol. 35, 286–304.
Taylor, M.A., 2012. Modelling travel time reliability with the burr distribution. Proc.-Soc. Behav. Sci. 54, 75–83.
Tu, H., Pel, A.J., Li, H., Sun, L., 2012. Travel time reliability during evacuation. Transp. Res. Rec.: J. Transp. Res. Board 2312 (1), 128–133.
Turner, S.M., Best, M.E., Schrank, D.L., 1996. Measures of effectiveness for major investment studies, Texas.
Van Lint, J., van Zuylen, H.J., Tu, H., 2008. Travel time unreliability on freeways: why measures based on variance tell only half the story. Transp. Res. Part A: Policy Practice 42 (1), 258–277.
van Lint, J.W., van Zuylen, H.J., 2005. Monitoring and predicting freeway travel time reliability: using width and skew of day-to-day travel time distribution. Transp. Res. Rec.: J. Transp. Res. Board 1917 (1), 54–62.
Wakabayashi, H., Iida, Y., 1992. Upper and lower bounds of terminal reliability of road networks: an efficient method with Boolean algebra. J. Natural Disaster Sci. 14 (1), 29–44.
Westfall, P.H., 1993. Resampling-Based Multiple Testing: Examples and Methods for *p*-value Adjustment. John Wiley & Sons.
Yao, B., Hu, P., Lu, X., Gao, J., Zhang, M., 2014. Transit network design based on travel time reliability. Transp. Res. Part C: Emerging Technol. 43, 233–248.
Yazici, M.A., Kamga, C., Mouskos, K.C., 2012. Analysis of travel time reliability in New York city based on day-of-week and time-of-day periods. Transp. Res. Rec.: J. Transp. Res. Board 2308 (1), 83–95.